Available online at www.sciencedirect.com
ScienceDirect
Ceramics International 34 (2008) 467–477
CERAMICS INTERNATIONAL
www.elsevier.com/locate/ceramint

Synthesis of nanosized PAA/titania hybrid composites—Experiment and modeling

Hung-Jen Chen [a], Leeyih Wang [b,c], Wen-Yen Chiu [a,b,*], Trong-Ming Don [d]

[a] Department of Chemical Engineering, National Taiwan University, Taiwan, ROC
[b] Institute of Polymer Science and Engineering, National Taiwan University, Taiwan, ROC
[c] Center for Condensed Matter Sciences, National Taiwan University, Taiwan, ROC
[d] Department of Chemical and Materials Engineering, Tamkang University, Taiwan, ROC

Received 30 January 2006; received in revised form 11 October 2006; accepted 22 November 2006
Available online 4 January 2007

Abstract

A stable colloid of nanosized PAA/titania hybrid has been successfully prepared, in which chelating bond was evidenced by FTIR spectra. Moreover, TGA curves indicated the degree of chelation to be increased with an increase of PAA content. SEM micrographs demonstrated that the size of hybrid aggregates would be smaller at increased ratio of PAA to titania, because the higher amount of PAA would decrease the degree of aggregation and inhibit the titania growth. A new sol–gel kinetic model for partially chelated titanium alkoxide by PAA has been proposed to simulate the experimental results. Based on this sol–gel kinetic model which takes into account the effect of chelation, the concentration of water, Ti–OR, Ti–OH, and (Ti–O)–Ti bonds during sol–gel reaction could be calculated. The variation of number of particles at different reaction times could also be shown. Finally, the size of hybrid aggregates at different degrees of chelation could be qualitatively described. The simulated results from this model were in agreement with the observation from SEM micrographs.

Keywords: Sol–gel reaction; Titania; Chelation; Kinetic simulation

1. Introduction

Over the past few years, considerable efforts have been made to prepare organic/inorganic hybrid materials. The main purpose is on the combination of properties of both materials such as flexibility, toughness, and easy processing of the organic component and hardness, strength, and thermal stability of the inorganic part. Under suitable conditions, the hybrid could exhibit better optical, electronic, optoelectronic, magnetic, mechanical, and thermal properties [1–9]. There are generally two methods to prepare organic/inorganic hybrids. One is the use of a coupling agent to combine the organic and inorganic moieties [1,2]. The other is the in situ sol–gel reaction generally used for metal alkoxides [3–5], especially for silica in the presence of an organic counterpart [6–9]. These approaches can give materials better performance due to sufficient chemical and interfacial bondings between the organic and inorganic components. From the point of processing, the in situ sol–gel reaction is more attractive due to its simple synthetic route.

Titania is of great interest as an inorganic phase due to its highly catalytic property, photostability, nontoxicity in addition to its low cost. The stability of titania colloidal solution is one of the important parameters in the manufacture of high-quality products such as cosmetics, paints, and ceramics [10,11]. However, the properties of organic/titania hybrid materials are hardly to manipulate because of the high reactivity of titanium alkoxide [12]. Therefore, acetic acid, a well known chelating agent for titanium alkoxide, is generally used to control the hydrolysis and polycondensation reactions [13,14].

Another chelating agent is poly(acrylic acid) (PAA), which could be strongly bounded to titania surface with the carboxylic acid group. Not only PAA could decrease the reactivity of titanium alkoxide but also increase the colloid stability due to the steric hindrance from polymer chains [11,14–16]. Accordingly, PAA has been widely applied in the preparation of titania

* Corresponding author at: Department of Chemical Engineering, National Taiwan University, No. 1, Sec. 4, Roosevelt Road, Taipei 106, Taiwan, ROC. Tel.: +886 2 23623259; fax: +886 2 23623259.
E-mail address: ycchiu@ntu.edu.tw (W.-Y. Chiu).

0272-8842/$34.00
doi:10.1016/j.ceramint.2006.11.013

Table 1
Composition and thermo properties of the prepared PAA/titania hybrid materials

Hybrid	[COOH]/[TIP] or ([COOH]/[TiOR]) (mole ratio)	Butanol (mole/l)	Experimental residual at 800 °C, ER (%)	Theoretical residual, TR (%)	Δ(ER-TR) (%)
A	5.04 (1.26)	10	42	17.35	24.65
B	6.72 (1.68)	10	38.8	13.61	25.19

A: [COOH] = 1.25 mole/l; [TIP] = 0.248 mole/l.
B: [COOH] = 1.25 mole/l; [TIP] = 0.186 mole/l.

colloidal solutions or porous titania films [11,16–19]. The aggregation of titania particles is generally ascribed to the London van der Wall force. Therefore, in order to provide particles stability, there must be a strong repulsive force among particles [20]. Three kinds of repulsive force could stabilize a suspension over the attractive force, namely, electrostatic, steric hindrance, and electrosteric. Boisvert et al. [16] proposed a theoretical model to investigate the effect of sodium polyacrylate on the rheological and packing behavior of concentrated suspensions.

Several factors such as size of aggregated particles and its distribution in the organic phase mainly control the performance of hybrid materials. Therefore, the development of a kinetic model will be beneficial for the prediction of the size of hybrid aggregates. The sol–gel mechanism of metal alkoxide, including hydrolysis, water condensation, and alcohol condensation, has been well studied [21,22]. However, the sol–gel mechanism for partially chelated titanium alkoxide has not been fully explored yet. In an effort to understand the sol–gel mechanism of partially chelated titanium alkoxide, a new sol–gel kinetic model is proposed in this study to describe the growth and aggregation of titania in the presence of PAA chelating agent. By considering reasonable values for all rate constants, this model can predict the effect of chelation on the size of hybrid aggregates very well; therefore providing useful information in designing a suitable reaction condition for the sol–gel reaction of titanium alkoxide.

2. Experimental

2.1. Materials

Poly(acrylic acid)(PAA) (Aldrich, $M_w = 2000$), titanium (IV) isopropoxide (TIP) (Acros, 98%) and 1-butanol (Acros, 99.5%) were used as received. The water used for the sol–gel reaction was purified by means of a Millipore Milli-Q system.

According to the molecular weight of PAA ($M_w = 2000$), 1 mole of PAA has about 27 equivalent moles of carboxylic acid groups. Two PAA/titania hybrids were prepared and their compositions based on molar ratio are listed in Table 1. For hybrid A, 2 ml of TIP was first dissolved in 25 ml of butanol. Subsequently, 2.5 g of PAA was added to the TIP solution and stirred 30 min. During the period of PAA dissolution, the solution became a light gel first and then gradually transformed to a clear solution. Then, the solution was heated to 90 °C, maintained at that temperature for 10 h. After that, the solution was cooled down to room temperature and a stable colloid was obtained. The synthetic route is shown in Fig. 1. In this method, the water was gradually generated from the esterification of PAA and butanol, thus providing a moderate rate for the sol–gel reaction. For hybrid B, the amount of TIP was decreased to be 1.5 ml, thus increasing the mole ratio of PAA to TIP, while the other conditions were the same.

2.2. Measurement methods

The functional groups and chelating behaviors of PAA and PAA/titania hybrids were analyzed by a Fourier transform infrared spectrophotometer (FTIR) (Bio-Rad, FTS-3000). The sample was prepared by mixing and grinding the hybrid with potassium bromide (KBr) and compressed into a pellet. The absorption spectra were recorded with 16 scans at a resolution of 4 cm^{-1} between 4000 and 400 cm^{-1}. A thermogravimetric analyzer (TGA) from Perkin-Elmer (TGA-7) was used to investigate the thermal degradation behavior of PAA and PAA/titania hybrids. Specimens of 5–15 mg ground powder were put into a platinum crucible and heated at a rate of 10 °C/min under nitrogen atmosphere. The recorded temperature was from 100

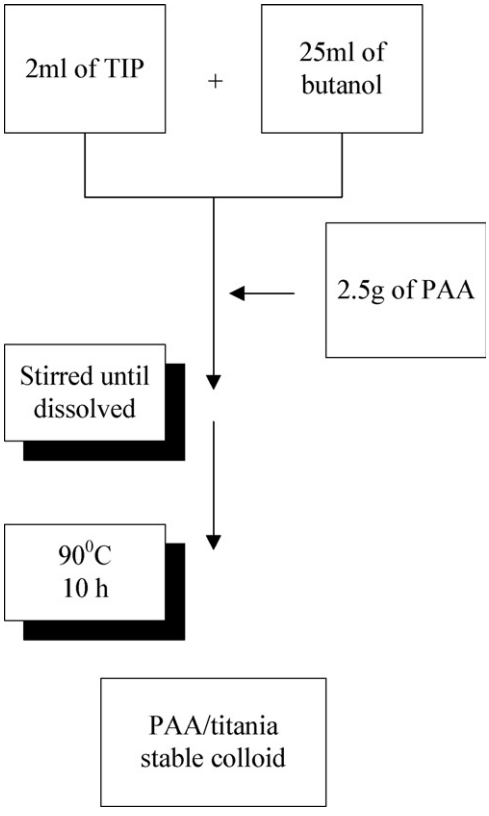

Fig. 1. In situ sol–gel process for the preparation of PAA/titania hybrid colloid.

to 800 °C. The aggregate size and aggregation phenomena of PAA/titania hybrids were observed by Hitachi (S-800) scanning electronic microscope (SEM) at an activation voltage of 20 kV.

3. Results and discussion

3.1. Chemical structures

FTIR spectra of the prepared PAA/titania hybrid materials and pure PAA are shown in Fig. 2. For pure PAA, the characteristic absorption band of carbonyl (C=O) was around 1699–1742 cm^{-1}, it was overlapped by the vibration of free state and self-associated dimmer by hydrogen bonding [23,24]. When the esterification was occurred, a relative sharp peak was observed at 1718 cm^{-1} for PAA/titania hybrids. From the literature, the free carbonyl vibration of poly methyl methacrylate (PMMA) was at 1730 cm^{-1}, whereas, this carbonyl vibration would shift to 1705 cm^{-1} when it had hydrogen bond with free carboxylic acid group of poly methacrylic acid (PMAA) [25]. It meant that the carbonyl vibration of ester group would shift from 1730 cm^{-1} to lower wave number as it had hydrogen bond with carboxylic acid group. It accounted that the co-existence of ester group and carboxylic acid group resulted in the carbonyl vibration of ester group was observed at 1718 cm^{-1}. In the same time, PAA/titania hybrid showed a new peak at 1560 cm^{-1}, indicating some of the carboxylic acid groups of PAA were chelated with titania. The ratio of the intensity of the chelating bond (1560 cm^{-1}) to that of the C=O bond (1718 cm^{-1}) was used to roughly estimate the ratio of the amount of chelated COOH to the amount of unchelated COOH, yielding the chelating efficiency. It should be mentioned that the unchelated COOH included free COOH and COOR formed from esterification. The results show that as the mole ratio of PAA to TIP increased, the efficiency of chelation was smaller due to the excess amount of free carboxylic acid groups.

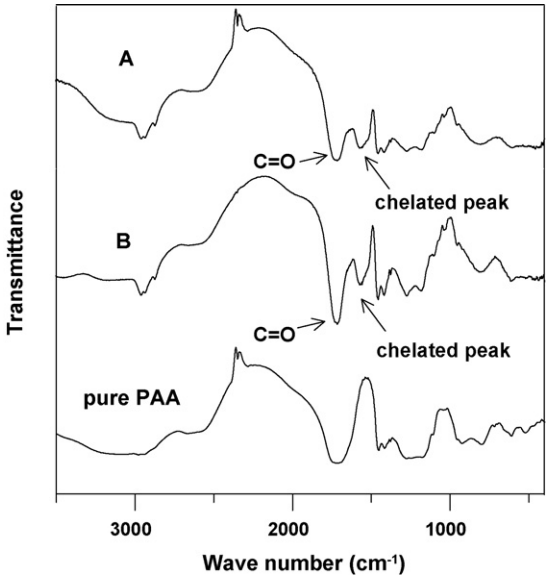

Fig. 2. FTIR spectra of the prepared hybrids and pure PAA.

3.2. Thermal degradation behavior

The TGA curves of PAA/titania hybrids with different amounts of TIP are shown in Fig. 3. As the mole ratio of PAA to TIP increased, both the thermal decomposition temperature (T_d) of PAA component and the residual weight were decreased. The residual weight of the prepared hybrids at 800 °C (ER) were given in Table 1, as well as the theoretical residual weight of hybrids at 800 °C (TR). The value of TR were calculated by assuming all of PAA were decomposed and the efficiency of titanium precursor transforming to titania was 100%, as represented in the following:

$$\text{theoretical residual (TR, \%)} = \frac{(\text{weight of TIP})(M_{TiO_2}/M_{TIP})}{(\text{weight of PAA}) + (\text{weight of TIP})(M_{TiO_2}/M_{TIP})}$$

where M_{TiO_2} and M_{TIP} were the molecular weight of TiO_2 and TIP, respectively.

The degree of chelation of titania with PAA was then assumed proportional to the difference between experimental and theoretical residual (Δ), and the values of Δ are listed in Table 1. As can be seen, the degree of chelation was enhanced with increasing the mole ratio of PAA to TIP. This is because if the relative amount of TIP was decreased, there would more opportunity for titania to chelate with PAA, resulting in the increase of the degree of chelation.

3.3. SEM observations of particles

The size of hybrid aggregates and degree of aggregation were observed from SEM micrographs. Fig. 4 shows the morphologies of the prepared hybrids. In comparison of hybrid A and B, the effect of the mole ratio of PAA to TIP on the size of hybrid aggregates and the degree of aggregation were clearly observed. As the mole ratio of PAA to TIP was increased, the size of hybrid aggregates became smaller and the degree of aggregation was lower.

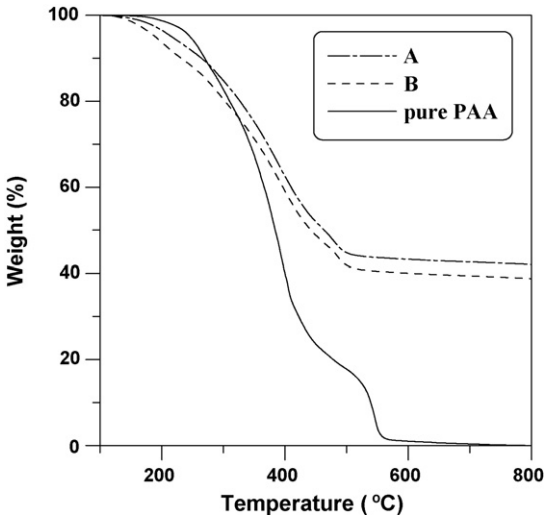

Fig. 3. TGA curves of the prepared hybrids and pure PAA.

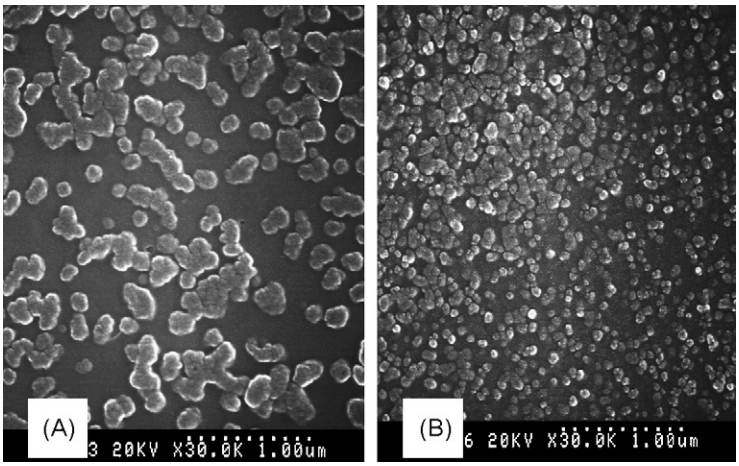

Fig. 4. SEM photographs of hybrids A and B.

When PAA was added to the TIP solution at room temperature, the solution became a light gel first and then gradually transformed to a clear solution. The formation of a light gel was due to the fact that the TIP was chelated with PAA and served as a gel point. When nanosized titania particles gradually formed, the conformation of PAA chains became more compactly adsorbing on the surfaces of nanoparticles, and the solution transformed to a clear solution. Then, the solution was heated to 90 °C and reaction was carried out at that temperature for 10 h. This process was to promote the water production from esterification of PAA and butanol, and then accelerated the sol–gel reaction of TIP. After the sol–gel reaction, this colloid solution could maintain its stable state at room temperature. This was attributed to the chelated PAA chains on the titania surface providing the effect of steric hindrance between particles that inhibited the aggregation of particles. In addition, the carboxylate anions (COO^-) of PAA chains over particle surfaces could also prevent particles from aggregation due to the electrostatic repulsion. Hence, the relatively high amount of PAA results in a high capability of anticoagulation, and also smaller size of particles. Beside the repulsive force caused by PAA chains, the higher amount of carboxylic acid groups chelated on TIP would also retard the hydrolysis of TIP and confine the growth of titania.

3.4. Kinetic model and simulation

3.4.1. Mechanism

For the titanium alkoxide system, the general chemical reactions which take place in the solution can be described as the following, including hydrolysis, water condensation, and alcohol condensation [21,22].

$$\text{hydrolysis}: \quad \underset{(y_1)}{\text{Ti}-\text{OR}} + \underset{(y_3)}{\text{H}_2\text{O}} \xrightarrow{k_{h1}} \underset{(y_4)}{\text{Ti}-\text{OH}} + \text{R}-\text{OH} \qquad \text{(i)}$$

water condensation

$$: \quad \underset{(y_4)}{\text{Ti}-\text{OH}} + \underset{(y_4)}{\text{Ti}-\text{OH}} \xrightarrow{k_{cw1}} \underset{(y_6)}{(\text{Ti}-\text{O})}-\text{Ti} + \underset{(y_3)}{\text{H}_2\text{O}} \qquad \text{(ii)}$$

alcohol condensation

$$: \quad \underset{(y_4)}{\text{Ti}-\text{OH}} + \underset{(y_1)}{\text{Ti}-\text{OR}} \xrightarrow{k_{ca1}} \underset{(y_6)}{(\text{Ti}-\text{O})}-\text{Ti} + \text{ROH} \qquad \text{(iii)}$$

In our system, several additional reactions must be considered due to the chelation of titanium alkoxide with carboxylic acid and esterification of PAA with butanol. In the following reactions, the notation of P represents PAA chains. First, titanium alkoxide and PAA may proceed in two kinds of reaction [25].

$$\text{chelation}: \quad \underset{(y_1)}{\text{Ti}-\text{OR}} + \underset{(y_8)}{\text{P}-\text{COOH}} \rightarrow \underset{(y_2)}{\text{Ti}-\text{OOC}-\text{P}} + \text{ROH} \qquad \text{(iv)}$$

$$\text{chelation}: \quad \underset{(y_1)}{\text{Ti}-\text{OR}} + \underset{(y_8)}{\text{P}-\text{COOH}} \rightarrow \underset{(y_5)}{\text{Ti}-\text{OH}} :: \text{ROOC}-\text{P} \qquad \text{(v)}$$

Then, the chelated titanium alkoxide (Ti–COO–P) can continue the following reactions [26].

$$\text{alcoholysis}: \quad \underset{(y_2)}{\text{Ti}-\text{OOC}-\text{P}} + \text{ROH} \rightarrow \underset{(y_5)}{\text{Ti}-\text{OH}} :: \text{ROOC}-\text{P} \qquad \text{(vi)}$$

$$\text{hydrolysis}: \quad \underset{(y_2)}{\text{Ti}-\text{OOC}-\text{P}} + \underset{(y_3)}{\text{H}_2\text{O}} \xrightarrow{k_{h2}} \underset{(y_5)}{\text{Ti}-\text{OH}} :: \underset{(y'_8)}{\text{HOOC}-\text{P}'} \qquad \text{(vii)}$$

$$\text{hydrolysis}: \quad \underset{(y_2)}{\text{Ti}-\text{OOC}-\text{P}} + \underset{(y_3)}{\text{H}_2\text{O}} \xleftarrow[k'_{h2}]{} \underset{(y_5)}{\text{Ti}-\text{OH}} :: \underset{(y'_8)}{\text{HOOC}-\text{P}'} \qquad \text{(viii)}$$

The notation of Ti–OH::ROOC–P and Ti–OH::HOOC–P meant that the generated Ti–OH had strong interaction with the neighboring PAA chains. In our system, reactions (v) and (vi) are minor compared to reactions (iv), (vii) and (viii). The following flow chart described the possible reactions of TIP and PAA, in which the dash lines meant the reactions being neglected in our kinetic simulation.

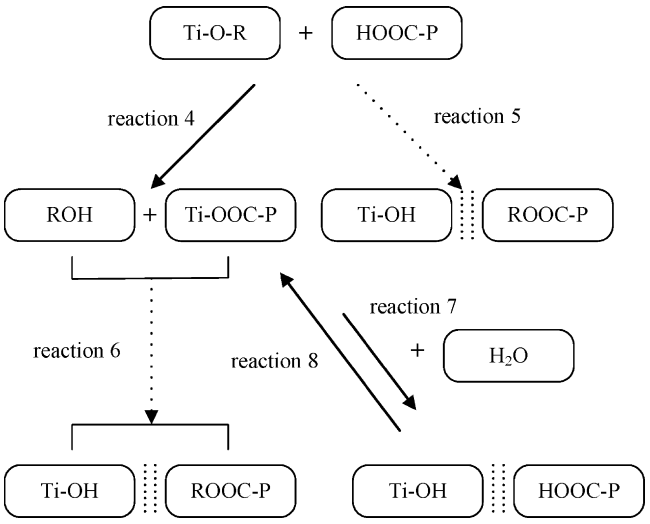

As the Ti–OH::HOOC–P was generated, the condensation for the growth of titania (TiO_2) would be proceeded subsequently. For simplifying the notation, the Ti–OH::HOOC–P or Ti–OH::ROOC–P was all substituted by Ti–OH::P and the notation of "::" meant strong interaction [25].

water condensation :

$$\underset{(y_5)}{\mathrm{Ti{-}OH}} :: \mathrm{P} + \underset{(y_4)}{\mathrm{Ti{-}OH}} \xrightarrow{k_{cw2}} \underset{(y_7)}{(\mathrm{Ti{-}O}){-}\mathrm{Ti}} :: \mathrm{P} + \underset{(y_3)}{\mathrm{H_2O}} \quad \text{(ix)}$$

water condensation :

$$\underset{(y_5)}{\mathrm{Ti{-}OH}} :: \mathrm{P} + \underset{(y_5)}{\mathrm{Ti{-}OH}} :: \mathrm{P} \xrightarrow{k_{cw3}} \underset{(y_7)}{(\mathrm{Ti{-}O}){-}\mathrm{Ti}} :: \mathrm{P} + \underset{(y_3)}{\mathrm{H_2O}} \quad \text{(x)}$$

alcohol condensation :

$$\underset{(y_5)}{\mathrm{Ti{-}OH}} :: \mathrm{P} + \underset{(y_1)}{\mathrm{Ti{-}OR}} \xrightarrow{k_{ca2}} \underset{(y_7)}{(\mathrm{Ti{-}O}){-}\mathrm{Ti}} :: \mathrm{P} + \mathrm{ROH} \quad \text{(xi)}$$

alcohol condensation :

$$\underset{(y_2)}{\mathrm{Ti{-}OOC{-}P}} + \underset{(y_4)}{\mathrm{Ti{-}OH}} \xrightarrow{k_{ca3}} \underset{(y_7)}{(\mathrm{Ti{-}O}){-}\mathrm{Ti}} :: \underset{(y_8'')}{\mathrm{HOOC{-}P''}} \quad \text{(xii)}$$

alcohol condensation :

$$\underset{(y_2)}{\mathrm{Ti{-}OOC{-}P}} + \underset{(y_5)}{\mathrm{Ti{-}OH}} :: \mathrm{P} \xrightarrow{k_{ca4}} \underset{(y_7)}{(\mathrm{Ti{-}O}){-}\mathrm{Ti}} :: \underset{(y_8'')}{\mathrm{HOOC{-}P''}} \quad \text{(xiii)}$$

And the esterification reactions of PAA and butanol were as below:

esterificaiton :

$$\underset{(y_8)}{\mathrm{P{-}COOH}} + \underset{(y_9)}{\mathrm{Bu{-}OH}} \xrightarrow{k_e} \mathrm{P{-}COOBu} + \underset{(y_3)}{\mathrm{H_2O}} \quad \text{(xiv)}$$

esterificaiton :

$$\underset{(y_8')}{\mathrm{P{-}COOH'}} + \underset{(y_9)}{\mathrm{Bu{-}OH}} \xrightarrow{k_e} \mathrm{P{-}COOBu'} + \underset{(y_3)}{\mathrm{H_2O}} \quad \text{(xv)}$$

esterificaiton :

$$\underset{(y_8'')}{\mathrm{P{-}COOH''}} + \underset{(y_9)}{\mathrm{Bu{-}OH}} \xrightarrow{k_e} \mathrm{P{-}COOBu''} + \underset{(y_3)}{\mathrm{H_2O}} \quad \text{(xvi)}$$

where y_1 is concentration of Ti–OR; y_2 the concentration of Ti–OOC–P; y_3 the concentration of H_2O; y_4 the concentration of Ti–OH; y_5 the concentration of Ti–OH::P; y_6 the concentration of (Ti–O)–Ti; y_7 the concentration of (Ti–O)–Ti::P; y_8 the concentration of P–COOH; $y_8'$the concentration of P–COOH′ released from reaction (vii); y_8'' the concentration of P–COOH″ released from reactions (xii) and (xiii); y_9 the concentration of butanol.

The condensation rate constant is defined as the rate constant associated with the transformation of one titanium hydroxyl functional group into the functional group represented by one of the titaniums present in the titanium–oxygen–titanium bond. Thus, for example, the condensation of two titanium hydroxyls to form one titanium–oxygen–titanium resulted in the formation of two condensation functional groups.

Both of the notations of (Ti–O)–Ti::P and (Ti–O)–Ti::HOOC–P represented the generated titania surrounded by PAA chains. Here, one assumption was made: the chelation reaction of titanium precursor with PAA [reaction (iv)] was instantaneous. The rate equations for different species in this reaction system can be expressed as follows:

$$\frac{dy_1}{dt} = -k_{h1}y_1y_3 - k_{ca1}y_4y_1 - k_{ca2}y_5y_1 \quad (1)$$

$$\frac{dy_2}{dt} = -k_{h2}y_2y_3 + k'_{h2}y_5y'_8 - k_{ca3}y_2y_4 - k_{ca4}y_2y_5 \quad (2)$$

$$\frac{dy_3}{dt} = -k_{h1}y_1y_3 + \frac{k_{cw1}}{2}y_4^2 - k_{h2}y_2y_3 + k'_{h2}y_5y'_8 + k_{cw2}y_5y_4 + \frac{k_{cw3}}{2}y_5^2 + k_ey_8y_9 + k_ey'_8y_9 + k_ey''_8y_9 \quad (3)$$

$$\frac{dy_4}{dt} = k_{h1}y_1y_3 - 2\frac{k_{cw1}}{2}y_4^2 - k_{ca1}y_4y_1 - k_{cw2}y_5y_4 - k_{ca3}y_2y_4 \quad (4)$$

$$\frac{dy_5}{dt} = k_{h2}y_2y_3 - k'_{h2}y_5y'_8 - k_{cw2}y_5y_4 - 2\frac{k_{cw3}}{2}y_5^2 - k_{ca2}y_5y_1 - k_{ca4}y_2y_5 \quad (5)$$

$$\frac{dy_6}{dt} = 2\frac{k_{cw1}}{2}y_4^2 + 2k_{ca1}y_4y_1 \quad (6)$$

$$\frac{dy_7}{dt} = 2k_{cw2}y_5y_4 + 2\frac{k_{cw3}}{2}y_5^2 + 2k_{ca2}y_5y_1 + 2k_{ca3}y_2y_4 + 2k_{ca4}y_2y_5 \quad (7)$$

$$\frac{dy_8}{dt} = -k_e y_8 y_9 \quad (8)$$

$$\frac{dy'_8}{dt} = k_{h2}y_2y_3 - k'_{h2}y_5y'_8 - k_e y'_8 y_9 \quad (9)$$

$$\frac{dy''_8}{dt} = k_{ca3}y_2y_4 + k_{ca4}y_2y_5 - k_e y''_8 y_9 \quad (10)$$

and $y_9 = y_{9,0}$.

These ordinary differential equations were solved by Mathematica program and executed by a Pentium IV–1.7G microprocessor. The initial conditions for y_1–y_9 and rate constants for kinetic modeling were listed in Table 2.

In our system, the chelation reaction of TiOR with PAA was found to occur very quickly. Similarly, the chelation reaction of TiOH with PAA [reaction (viii)] should be fast. From literature, for silicon alkoxide [$Si(OCH_3)_4$] [27], the hydrolysis rate constant was about 0.2 l/(mole min); water condensation and alcohol condensation rate constants were 0.006 and 0.001 l/(mole min), respectively. It is known that the rate constants of hydrolysis, water condensation, and alcohol condensation for titanium alkoxide are all much larger than those in silicon alkoxide, so they were assumed as 100 times of those values in silicon alkoxide system as listed in Table 2. However, if the titanium alkoxide was chelated with carboxylic acid, the rate constant would be much smaller than those that were not chelated. Moreover, the reactivity of TiOH::P was assumed smaller than free TiOH because its reactivity will be influenced by the steric hindrance of PAA chains. As for the rate constant of the reaction of chelated titanium alkoxide and TiOH::P, it was smaller than the rate constant of free TiOR and TiOH four orders of magnitude. In the esterification, the concentration of butanol solvent was taken to be constant and its rate constant was set as 1.0×10^{-4} l/(mole min) [28].

3.4.2. Nucleation of particles

At the beginning, all reactions, including hydrolysis and condensation, occurred in a homogenous system and the rate constants were assumed to be constant. As reaction proceeded, nucleation of particles occurred and the reactions started to occur in a heterogeneous system. The rate constant would gradually decrease due to the increase in difficulties for reactions to occur between functional groups on particle surfaces. Hence, we assumed that all rate constants, except k_e, were constant at the initial stage of reaction and then decreased obviously when the reaction reached a critical extent of reaction, P_c. The definition of extent of reaction will be discussed later. At the same time, a hypothesis was made that the formation of new nuclei would no longer occur, when the reaction reached this critical extent of reaction. Thus no more nucleation of particles was expected and the reactions would occur either between sol and particle or between particles when the concentration of particles reached a certain high level.

In order to determine the critical extent of reaction P_c and thus the critical reaction time t_0, two new parameters are defined:

Extent of reaction, P:

$$P = \frac{y_6 + y_7}{y_{1,0} + y_{2,0}} \quad (11)$$

where $y_{1,0}$ is initial concentration of Ti–OR bonds; $y_{2,0}$ is initial concentration of Ti–OOC–P bonds.

Degree of polymerization for titanium precursor $Ti(OR)_4$, X_n:

$$X_n = \frac{(1/4)(y_{1,0} + y_{2,0})}{(1/4)(y_{1,0} + y_{2,0}) - (1/2)(y_6 + y_7)} \quad (12)$$

Table 2
Initial conditions of cases I–III, parameters, and rate constants for kinetic modeling

Case	$[COOH]_{t,0}/[Ti–OR]_{t,0}$	Degree of chelation $[P–Ti–OR]_0/[Ti–OR]_{t,0}$	t_0 (min)	$k_{a,0}$ (l/(mole min))	$y_{1,0}$ (mole/l)	$y_{2,0}$ (mole/l)	$y_{8,0}$ (mole/l)	$y_{9,0}$ (mole/l)	$y_{3,0}$–$y_{7,0}$, $y'_{8,0}$, $y''_{8,0}$ (mole/l)
I	1	1/8	331	0.1	1.4	0.2	1.4	10	0
II	2	2/8	163	0.05	1.2	0.4	2.8	10	0
III	4	3/8	86	0.001	1.0	0.6	5.8	10	0

Rate constants	k_0 in Eq. (16) (l/(mole min))	Assumption
$k_{h1,0}$	20	$100 \times (k_h$ of $Si(OCH_3)_4)$ [23]
$k_{h2,0}$	0.02	$10^{-3} \times k_{h1,0}$
$k'_{h2,0}$	10	
$k_{cw1,0}$	0.6	$100 \times (k_{cw}$ of $Si(OCH_3)_4)$ [23]
$k_{cw2,0}$	0.06	$0.1 \times k_{cw1,0}$
$k_{cw3,0}$	0.012	$0.02 \times k_{cw1,0}$
$k_{ca1,0}$	0.1	$100 \times (k_{ca}$ of $Si(OCH_3)_4)$ [23]
$k_{ca2,0}$	0.01	$0.1 \times k_{ca1,0}$
$k_{ca3,0}$	0.0001	$10^{-3} \times k_{ca1,0}$
$k_{ca4,0}$	0.00001	$10^{-4} \times k_{ca1,0}$
k_e	0.0001	Constant throughout the reaction

$[Ti–OR]_{t,0} = [Ti–OR]_0 + [Ti–OOC–P]_0 = y_{1,0} + y_{2,0}$; $[COOH]_{t,0} = [COOH]_0 + [Ti–OOC–P]_0 = y_{8,0} + y_{2,0}$; $k_b = 1$ (constant throughout the reaction); $k_D = 16$ (nm).

From Eqs. (11) and (12), we obtained

$$X_n = \frac{1}{1-2P} \tag{13}$$

According to the statistical approach [29], the critical extent of reaction P_c is defined as below, which is the lower bound of P_c to form gelation:

$$P_c = \frac{1}{f-1} = \frac{1}{3} \tag{14}$$

In Eq. (14), f is the functionality of reactants and the value of f was taken as 4 in our system. Thus, Eq. (14) gives $P_c = 1/3$, and in turn by substituting this value into Eq. (13), $X_{nc} = 3$. Therefore, at the beginning of gel formation, the degree of polymerization of titanium precursor was 3. It meant that when the size of titania reached the dimension of 12 Ti–O bonds, nucleation of particles began to occur.

On the other hand, according to Carother's equation [28], the critical extent of reaction at gelation, P_c, is derived as below, which is the upper bound of P_c:

$$P_c = \frac{2}{f} - \frac{2}{\overline{X_n} f} = \frac{2}{f} = \frac{1}{2} \quad \text{as } X_n \to \infty \tag{15}$$

From Eq. (15), the critical extent of reaction P_c was over-estimated as 1/2 due to the assumption of $X_n \to \infty$ at gelation.

As a result, the critical extent of reaction at gelation in a real system was supposed to lie somewhere between 1/3 and 1/2. If the critical extent of reaction was assumed as 0.475, i.e., the critical degree of polymerization X_{nc} was 20. Hence, all rate constants could be expressed by the following equation, using k to represent all of the rate constants, except k_e.

$$k = k_0[U(p[t]) - U(p[t] - 0.475)] + k_0 \exp[-10(p[t] - 0.475)][U(p[t] - 0.475)]. \tag{16}$$

As $P \le P_c$ or $t \le t_0$, k was a constant; as $P > P_c$ or $t > t_0$, k value decreased in an exponential decay, where k_0 was the initial rate constant of k, and U meant unit step function.

In the above rate equations, all the concentrations of different species represent single bond concentrations such as Ti–OR, Ti–OH, and (Ti–O)–Ti. Three cases to describe how the degree of chelation on TIP affected the size of aggregated particles were considered. Previously, it was already shown that the degree of chelation on TIP increased with increasing the ratio of PAA/TIP. In case I, the mole ratio of unchelated TIP to chelated TIP was set at 7, when the concentration ratio of Ti–OR to COOH was 1–4. In the other two cases, case II and case III, the mole ratio of unchelated TIP to chelated TIP was 6:2 and 5:3, respectively, where the concentration ratio of Ti–OR to COOH was 1:2 and 1:4, respectively. The conditions for these three cases are listed in Table 2, where the degree of chelation was increased from 1/8 to 3/8, accordingly.

Fig. 5 shows the variation of extent of reaction P with time. It is shown that by setting P_c as 0.475, the critical time t_0 could be determined, which decreased from case I to case III. The values are listed in Table 2. Among three cases, case III gives the highest rate in water generation, and thus the largest amount of water, because the addition of PAA was the largest. Consequently, the critical time to reach P_c was the smallest. Fig. 6 shows the degree of polymerization X_n with extent of reaction P. According to Eq. (13), the relationship of X_n versus P would not be different for these three cases having different degree of chelation. Therefore, they are all on the same curve as shown in Fig. 6. In corresponding to the experimental results, the initial concentration of water was zero and the source of water only came from esterification.

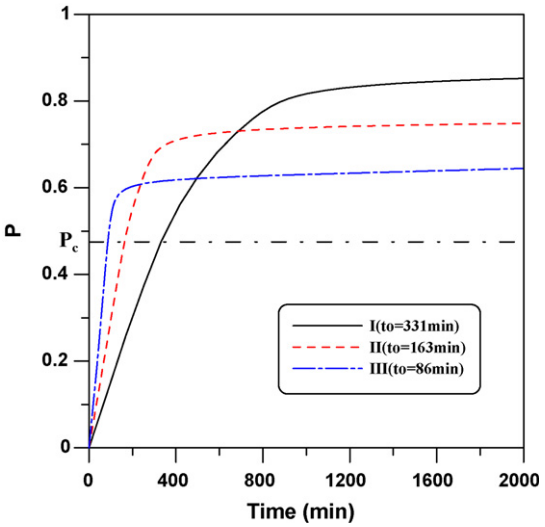

Fig. 5. Extent of reaction P vs. time. In this work, $P_c = 0.475$, $t_{0(I)} = 331$ min, $t_{0(II)} = 163$ min, $t_{0(III)} = 86$ min.

Fig. 7 shows the concentration variation of Ti–OR and Ti–OOC–P with time. It showed that the concentration of Ti–OOC–P remained high and the concentration of Ti–OR decreased in a faster rate as the concentration of PAA was increased. This was because the higher concentration of PAA gave the higher generation rate and thus the larger amount of water, as shown in Fig. 8. The produced water further caused

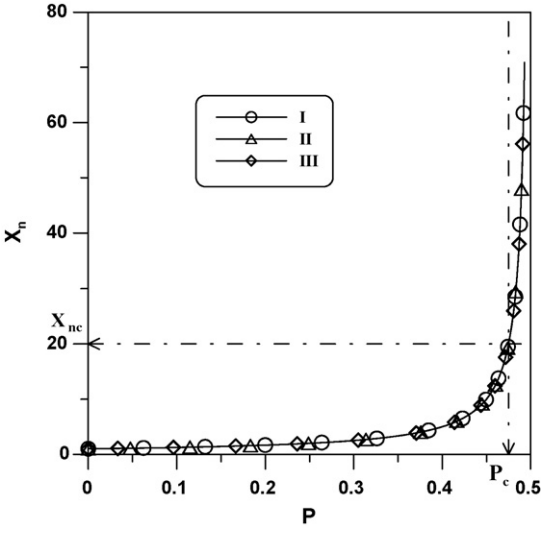

Fig. 6. Relationship between degree of polymerization X_n and extent of reaction P for cases I–III. In this work, $P_c = 0.475$, $X_{nc} = 20$.

the hydrolysis reaction of Ti–OR to Ti–OH. Consequently, a higher increasing rate in the concentration of Ti–OH and Ti–OH::P was observed in Fig. 9(a) and (b) when the concentration of PAA was higher. However, as the concentration of Ti–OH reached a maximum value, it then decreased gradually due to the condensation reactions of Ti–OH to (Ti–O)–Ti. Because the rate constant of Ti–OH was larger than that of Ti–OH::P, most of the condensation was thus resulted from the reaction of Ti–OH.

Fig. 10(a) and (b) shows the concentration variation of (Ti–O)–Ti and (Ti–O)–Ti::P bonds with time. In the early stage of reaction, the formation of (Ti–O)–Ti and (Ti–O)–Ti::P bonds were faster for case III than case I, because the higher formation rate of Ti–OH bonds in case III. However, when the reaction continued, the effect of chelation became obvious. The sol–gel reaction and the formation of (Ti–O)–Ti bonds would be inhibited and confined as the degree of chelation was increased. As a result, the overall concentration of (Ti–O)–Ti bonds, including (Ti–O)–Ti and (Ti–O)–Ti::P bonds, was higher for case I than case III. Most concentration of Ti–O bonds came from (Ti–O)–Ti bonds because the reactivities of Ti–OR and Ti–OH were higher than Ti–OOC–P and Ti–OH::P

3.4.3. Concentration and size of aggregated particles

In addition, two equations were formulated in order to simulate the growth of aggregated particles. Eq. (17) was to simulate the concentration of aggregated particles, N. Eq. (19) was to simulate the growth of average size of aggregated particles, D. Two factors were considered to have influence on the concentration of aggregated particles. In Eq. (17), the first term was the decrease of particle number caused by the chemical reaction or physical aggregation between particles, which was induced by a lot of hydroxyl and alkoxide groups on the titania surface. The second term represented the increase of particle number during the period of particle nucleation, $t \leq t_0$. The rate of nucleation was assumed to be proportional to the rate of formation of (Ti–O)–Ti bonds but ceased after a critical time, t_0. The definition of critical time t_0 was discussed previously. Therefore, the rate equation of N is represented as:

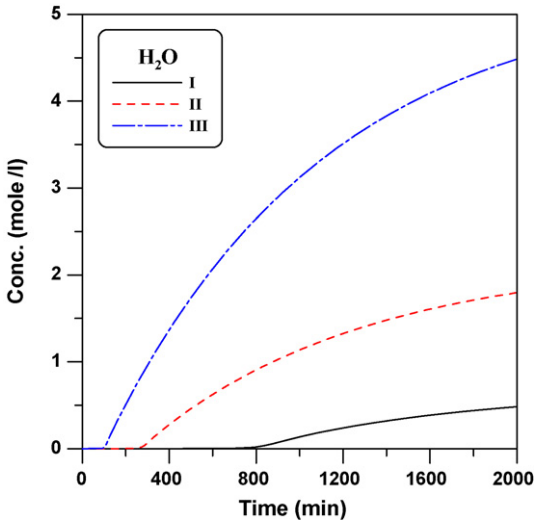

Fig. 8. Concentration vs. time for H_2O.

$$\frac{dN}{dt} = -k_a N^2 + k_b \left[\frac{dy_6}{dt} + \frac{dy_7}{dt}\right][U(t) - U(t - t_0)] \quad (17)$$

As mentioned in SEM section, the higher mole ratio of PAA to TIP provided higher ability of repulsive force between particles, thus decreasing the degree of aggregation. Hence, the rate constant value of k_a was decreased from cases I to III, as listed in Table 2. The degree of chelation on titania increased from I to III with increasing the mole ratio of PAA to TIP. It should be noticed that the rate constant of k_b was assumed constant and k_a, rate constant of aggregation would decay when the reaction reached a critical extent of reaction, P_c, just as the rate constant of hydrolysis and condensation.

$$k_a = k_{a,0}[U(p[t]) - U(p[t] - 0.475)] + k_{a,0}\exp[-100(p[t] - 0.475)][U(p[t] - 0.475)]. \quad (18)$$

Fig. 11 shows the concentration of aggregated particles with reaction time. It shows that the concentration of particles

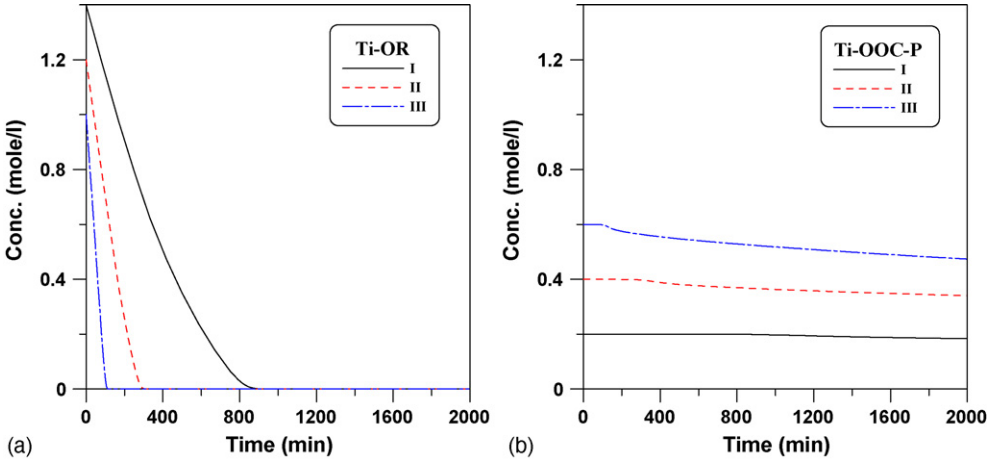

Fig. 7. Concentration vs. time for: (a) unchelated Ti–OR and (b) chelated Ti–OOC–P.

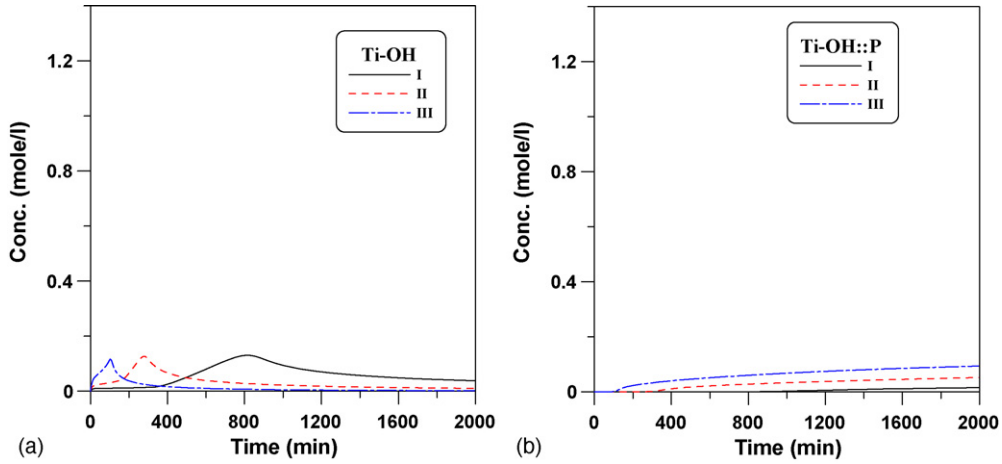

Fig. 9. Concentration vs. time: (a) for Ti–OH and (b) for Ti–OH::P.

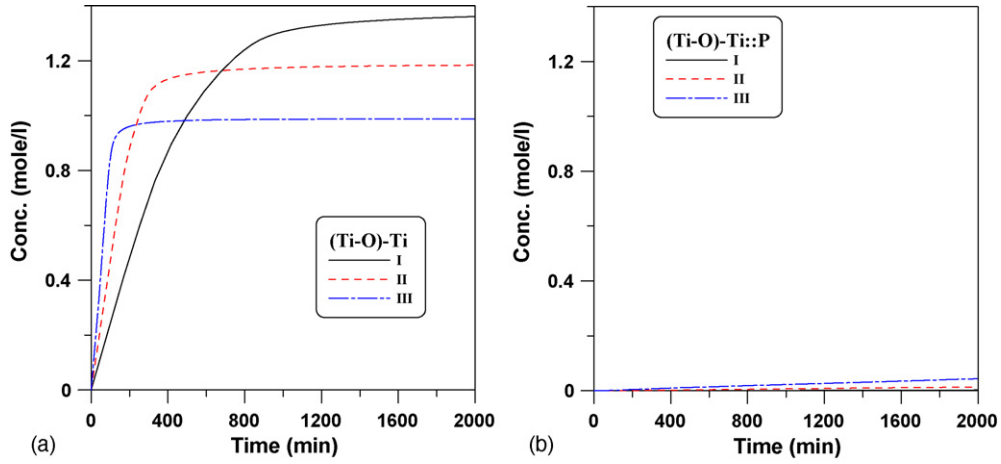

Fig. 10. Concentration vs. time: (a) for (Ti–O)–Ti and (b) for (Ti–O)–Ti::P.

reached higher value in the reaction system, with higher mole ratio of PAA to TIP.

Finally, the average size of aggregated particles D was defined as:

$$D = k_{\mathrm{D}} \frac{y_6 + y_7}{N}. \tag{19}$$

It meant that the average size of aggregated particles was proportional to the overall concentration of (Ti–O)–Ti bonds, including (Ti–O)–Ti and (Ti–O)–Ti::P bonds, divided by the concentration of aggregated particles. The unit of D was nanometer (nm) and k_{D} was a proportional constant. Fig. 12 shows the simulated average size of aggregated particles for the systems with different mole ratios of $[\mathrm{COOH}]_{t,0}$ to $[\mathrm{TIP}]_{t,0}$. It was clearly observed that if the mole ratio of $[\mathrm{COOH}]_{t,0}$ to $[\mathrm{TIP}]_{t,0}$, thus degree of chelation, was higher, the average size of aggregated particles was smaller. The steady state values of D form Fig. 12 were rearranged in Fig. 13 for different mole ratios of [COOH]/[TIP] in cases I–III. The sizes of aggregated particles of hybrids A and B from SEM measurement were also shown in Fig. 13 for comparison. The size of hybrid A ranged from 100 to 150 nm whereas the size of hybrid B ranged from 70 to 90 nm as seen in Fig. 13. This simulated result agreed with the SEM observation. It was concluded that this model can reasonably predict the experimental results of the sol–gel reaction of TIP in butanol with PAA as a chelating agent.

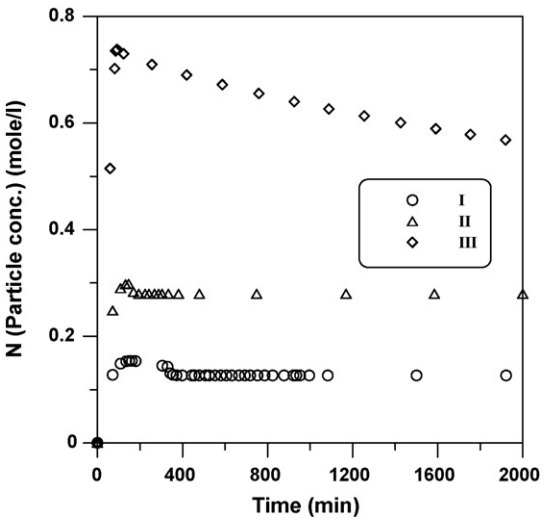

Fig. 11. Concentration variation of aggregated particles for cases I–III.

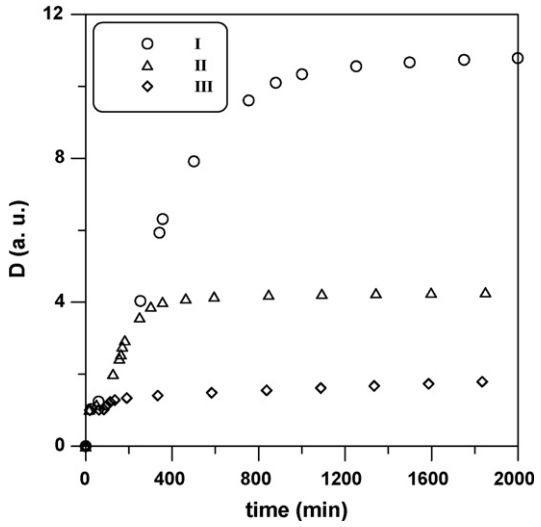

Fig. 12. Growth of average size of aggregated particles D for cases I–III.

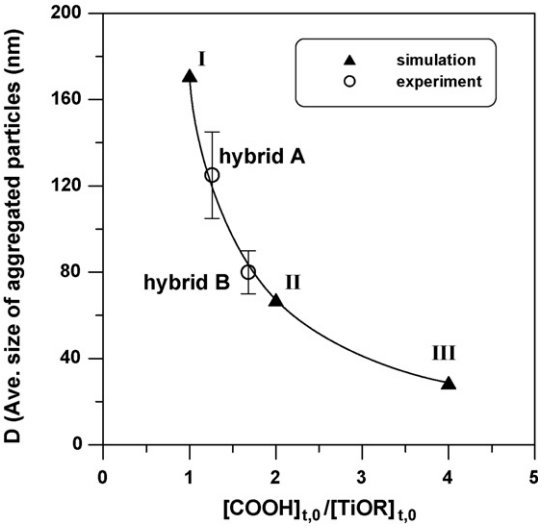

Fig. 13. Simulated relationship of average size of aggregated particles D and mole ratio of $[COOH]_{t,0}$ to $[TIP]_{t,0}$ for cases I–III. Experimental average particle size was fitted on the simulated curve.

4. Conclusions

A reaction mechanism was proposed for a sol–gel reaction of titanium alkoxide in the presence of PAA, where titanium alkoxide was partially chelated. Based on this new mechanism, a kinetic model was developed to simulate the concentration of reaction species and the growth of aggregated particles. The average size of aggregated particles decreased as the degree of chelation on TIP increased.

The chelating bond between PAA chains and titania was confirmed from FTIR spectra. The degree of chelation was increased with increasing the mole ratio of PAA to TIP, as revealed by TGA results. Based on SEM photographs, the degree of aggregation and the size of aggregated particles were found to be affected by the degree of chelation by changing the mole ratio of PAA to TIP. The results of simulated average size of aggregated particles, D, from the kinetic model agreed very well with the experimental observations.

References

[1] W.J.E. Beek, R.A.J. Janssen, Photoinduced electron transfer in hetero-supramolecular assemblies of TiO_2 nanoparticles and terthiophene carboxylic acid in apolar solvents, Adv. Funct. Mater. 12 (8) (2002) 519–525.
[2] E.J. Nassar, R.R. Goncalves, M. Ferrari, Y. Messaddeq, S.J.L. Ribeiro, Titania-based organic–inorganic hybrid planar waveguides, J. Alloys Compd. 344 (1/2) (2002) 221–225.
[3] S. Roux, G.J.A.A. Soler-Illia, S. Demoustier-Champagne, P. Audebert, C. Sanchez, Titania/polypyrrole hybrid nanocomposites built from in-situ generated organically functionalized nanoanatase building blocks, Adv. Mater. 15 (3) (2003) 217–221.
[4] P.C. Chiang, W.T. Whang, The synthesis and morphology characteristic study of BAO-ODPA polyimide/TiO_2 nano hybrid films, Polymer 44 (8) (2003) 2249–2254.
[5] L. Liu, Q.H. Lu, J. Yin, X.F. Qian, W.K. Wang, Z.K. Zhu, Z.G. Wang, Photosensitive polyimide (PSPI) materials containing inorganic nano particles (I)PSPI/TiO_2 hybrid materials by sol–gel process, Mater. Chem. Phys. 74 (2) (2002) 210–213.
[6] R.L. Ballard, S.J. Tuman, D.J. Fouquette, W. Stegmiller, M.D. Soucek, Effects of an acid catalyst on the inorganic domain of inorganic–organic hybrid materials, Chem. Mater. 11 (3) (1999) 726–735.
[7] T.C. Chang, Y.T. Wang, Y.S. Hong, Y.S. Chiu, Organic–inorganic hybrid materials. V. Dynamic and degradation of poly(methyl methacrylate) silica hybrids, J. Polym. Sci., Part A: Polym. Chem. 38 (11) (2000) 1972–1980.
[8] M.I. Sarwar, Z. Ahmad, Interphase bonding in organic–inorganic hybrid materials using aminophenyltrimethoxysilane, Eur. Polym. J. 36 (1) (2000) 89–94.
[9] C.J.T. Landry, B.K. Coltrain, J.A. Wesson, N. Zumbulyadis, J.L. Lippert, *In situ* polymerization of tetraethoxysilane in polymers: chemical nature of the interactions, Polymer 33 (7) (1992) 1496–1506.
[10] R.R. Blaskey, J.E. Hall, in: P.A. Lewis (Ed.), Pigment Handbook, vol. 1, Wiley, New York, 1988, p. 1.
[11] S. Liufu, H. Xiao, Y. Li, Adsorption of poly(acrylic acid) onto the surface of titanium dioxide and the colloidal stability of aqueous suspension, J. Colloid Interf. Sci. 281 (1) (2005) 155–163.
[12] B.M. Novak, Hybrid nanocomposite materials—between inorganic glasses and organic polymers, Adv. Mater. 5 (6) (1993) 422–433.
[13] S. Doeuff, M. Henry, C. Sanchez, J. Livage, Hydrolysis of titanium alkoxides: modification of the molecular precursor by acetic acid, J. Non-Cryst. Solids 89 (1–3) (1987) 206–216.
[14] J. Zhang, S.C. Luo, L. Gui, Poly(methyl methacrylate)-titania hybrid materials by sol–gel processing, J. Mater. Sci. 32 (5/6) (1997) 1469–1472.
[15] H.J. Chen, P.C. Jian, J.H. Chen, L. Wang, W.Y. Chiu, Nanosized-hybrid colloids of Poly(acrylic acid)/Titania prepared via in-situ Sol-Gel reaction, Ceramics Int.
[16] J.P. Boisvert, J. Persello, J.C. Castaing, B. Cabane, Dispersion of alumina-coated TiO_2 particles by adsorption of sodium polyacrylate, Colloids Surf. A 178 (1–3) (2001) 187–198.
[17] M. Breulmann, S.A. Davis, S. Mann, H.P. Hentze, M. Antonietti, Polymer-gel templating of porous inorganic macro-structures using nanoparticles building blocks, Adv. Mater. 12 (7) (2000) 502–507.
[18] J.A. He, R. Mosurkal, L.A. Samuelson, L. Li, J. Kumar, Dye-sensitized solar cell fabricated by electrostatic layer-by-layer assembly of amphoteric TiO_2 nanoparticles, Langmuir 19 (6) (2003) 2169–2174.
[19] J. Huang, I. Ichinose, T. Kunitake, A. Nakao, Preparation of nanoporous titania films by surface sol–gel process accompanied by low-temperature oxygen plasma treatment, Langmuir 18 (23) (2002) 9048–9053.
[20] C.S. Hirtzel, R. Rajagopalan, Invited review stability of colloidal dispersions, Chem. Eng. Commun. 33 (5/6) (1985) 301–324.
[21] C.J. Brinker, G.W. Scherer, Sol Gel Science, Academic Press, 1990.

[22] B.E. Yoldas, Hydrolysis of titanium alkoxide and effects of hydrolytic polycondensation parameters, J. Mater. Sci. 21 (3/4) (1986) 1087–1092.
[23] J. Dong, Y. Ozaki, K. Nakashima, Infrared, Raman, and Near-Infrared spectroscopic evidence for the coexistence of various hydrogen-bond forms in poly(acrylic acid), Macromolecules 30 (4) (1997) 1111–1117.
[24] H.R. Motzer, P.C. Painter, M.M. Coleman, Interactions in miscible blends of poly(styrene-*co*-methacrylic acid) with copolymers containing vinylpyrrolidone and vinylpyridine groups, Macromolecules 34 (23) (2001) 8390–8393.
[25] S.W. Kuo, F.C. Chang, Miscibility and hydrogen bonding in blends of poly(vinylphenol-*co*-methyl methacrylate) with poly(ethylene oxide), Macromolecules 34 (12) (2001) 4089–4097.
[26] D.P. Birnie, Esterification kinetics in titanium isopropoxide-acetic acid solutions, J. Mater. Sci. 35 (2) (2000) 367–374.
[27] R.A. Assink, B.D. Kay, Sol–gel kinetics. I. Functional group kinetics, J. Non-Cryst. Solids 99 (1988) 359–370.
[28] P.J. Flory, Principles of Polymer Chemistry, Cornell University Press, Ithaca, NY, 1953, pp. 70–71.
[29] G. Odian, Principles of Polymerization, 3rd ed., Wiley, New York, 1991, pp. 110.